Free-Space-Optical Mobile Ad Hoc Networks: Auto-Configurable Building Blocks

Murat Yuksel, Jayasri Akella, Shivkumar Kalyanaraman, Partha Dutta

Rensselaer Polytechnic Institute, ECSE Department, JEC 6049

110 8th Street, Troy, NY 12180, USA.

Phone: +1 (518) 276 6823, Fax: +1 (925) 888 2167

Emails: **yuksem@ecse.rpi.edu**, **akellj@rpi.edu**, **shivkuma@ecse.rpi.edu**, **duttap@rpi.edu**

Abstract- **Existence of line of sight (LOS) and alignment between the communicating antennas is one of the key requirements for free-space-optical (FSO) communication. To ensure uninterrupted data flow, auto-aligning transmitter and receiver modules are necessary. We propose a new FSO node design that uses spherical surfaces covered with transmitter and receiver modules for maintaining optical links even when nodes are in relative motion. The spherical FSO node provides angular diversity in 3-dimensions, and hence provides an LOS at any orientation as long as there are no obstacles in between the communicating nodes. For proof-of-concept, we designed and tested an auto-configurable circuit, integrated with light sources and detectors placed on spherical surfaces. We demonstrated communication between a stationary and a mobile node using these initial prototypes of such FSO structures. We also performed the necessary theoretical analysis to demonstrate scalability of our FSO node designs to longer distances as well as feasibility of denser packaging of transceivers on such nodes.**

Keywords- **Free Space Optical communication, Auto-Configurable, Angular Diversity.**

I. INTRODUCTION

Optical wireless, also known as free space optics (FSO), is an effective high bandwidth communication technology serving commercial point-to-point links in terrestrial last mile applications and in infrared indoor LANs [27] [11] [1] [28] [13] [3]. FSO has several attractive characteristics like license-free band of operation, dense spatial reuse, low power usage per transmitted bit, and relatively high bandwidth. However, one of the major limitations of FSO is

line of sight (LOS) maintenance for continuous data flow. Current FSO equipment is targeted at point-to-point links using high-powered lasers and relatively expensive components used in fiber-optical transmission. Mobile communication using FSO is considered for indoor environments, within a single room, using diffuse optics technology [13] [11] [8] [18] [24] [30] [7]. Due to limited power of a single source that is being diffused to spread in all directions, these techniques are suitable for small distances (typically 10s of meters), but not suitable for longer distances. For outdoors, fixed FSO communication techniques to remedy small vibrations [4] [5], swaying of the buildings have been implemented using mechanical auto-tracking [6] [2] [17] or beam steering [29], and interference [16] and noise [26]. Similarly, for optical interconnects, auto-alignment or wavelength diversity techniques are reported to improve the misalignment tolerances in 2-dimensional arrays [19] [12] [9] [10] [14]. These techniques work only over small ranges (e.g. 1μm – 1 cm) and some of these are cumbersome involving heavy mechanical tracking instruments. Moreover, they are designed to improve the tolerance to movement and vibration but not to handle mobility. Thus, *mobile* FSO communication has not been realized, particularly for ad hoc networking and communication environments.

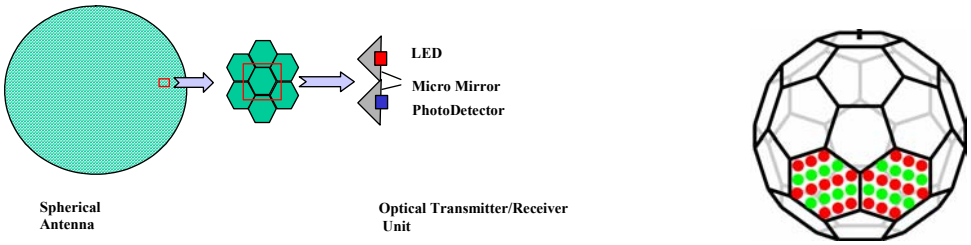

(a) Tessellated sphere **(b) Honeycombed arrays of transceivers**

Figure 1: 3-d spherical FSO systems tessellated with LED+PD pairs: Spherical surface provides angular diversity and nice coverage with almost omni-directional LOS capabilities. Dense packaging of transceivers using cheap optoelectronic components as well as both single and arrays of such transceivers on honeycombed cells are possible.

In order to enable FSO communication in mobile environments, we introduce the concept of spherical FSO node that provides angular diversity and hence LOS in all directions. Figure 1 shows the general concept of spherical surfaces being tessellated with FSO transceivers, i.e. a pair

of optical transmitter (e.g. Light Emitting Diode (LED)) and optical receiver (e.g. Photo-Detector (PD)). Such spherical FSO nodes use multiple optical transceivers tessellated on the surface of a sphere. The tessellation not only improves the range characteristics because every direction now has a light source (e.g. an LED) whose operating range is typically up to a few hundred meters, but also enables multi-channel simultaneous communication through multiple transceivers. As shown in Figure 1-(b), tradeoffs between spatial reuse and angular diversity can be obtained by constructing the FSO node as honeycombed arrays of transceivers where each array is a cell on the honeycomb.

In this paper, to illustrate feasibility of above-mentioned spherical FSO nodes, we design an auto-alignment circuit that electronically tracks the light beams to maintain continuous LOS between two communicating optical nodes even when they are mobile, and demonstrate the mobility in a two-node proto-type experiment.

We also show through theoretical modeling that these FSO node designs can allow very dense packaging and scale to very long communication ranges as well as coverage (e.g. a 1cm radius FSO node with transceivers of radius 0.1cm and source power 32mWatts can cover a total of 2272.68m^2 in adverse weather and 5230.97m^2 in clear weather). Our modeling of the proposed spherical FSO node revealed that the source power at transmitters and the visibility have little or no effect on the optimality of the number of transceivers on such structures. Rather, the geometric shape of the FSO node and the divergence angle play the major role, which means that adaptive tuning of the source power based on the actual visibility is possible without having to change the physical number of transceivers on these FSO nodes. This is an important result since it means that optimum number of transceivers is *fixed* for a particular FSO node design. *To the best of our knowledge, this is the first time spatial reuse and angular diversity coupled with electronic tracking (i.e. auto-alignment) for "mobile" communications using free space optical technology is being reported.*

II. BACKGROUND

Though some preliminary multi-hop proposals exist, current FSO equipment is targeted at point-to-point links using high-powered lasers and relatively expensive components used in fiber-optical transmission. The focus of these commercial systems (e.g. Terabeam [25] & LightPointe [15]) is to form a single primary beam (and some backup beams) with limited spatial re-use/redundancy and to push the limits of operating range, and to improve link availability during poor conditions [19]. We instead, focus on solving the LOS alignment problem with dense packaging of transceiver elements, enabling mobility through circular or spherical auto-configuring FSO systems, and targeting shorter per hop distances.

In commercial FSO systems, lasers in the 850nm and 1550nm band are preferred due to superior propagation characteristics in this band and higher power budget due to low geometric dispersion. Such equipment would be very costly and demands high-power in the context of multi-element scenario. Moreover, such laser-based equipment would not have the form factor, weight and power characteristics to be mounted on ad-hoc infrastructures. We, instead, investigate FSO systems using models of LEDs in our design as they are more amenable to dense and spatial packaging, and have longer life than lasers and fewer eye-safety regulations.

High-brightness LED technology is being rapidly developed in the context of solid-state lighting [28] [23]. Similarly, VCSELs are also very low-cost and provide high reliability. VCSELs and LEDs can be internally modulated at rates up to 2Gbps [11], and spatial packaging of hundreds of such devices can yield very high aggregate transmission capacities. Recently, wireless communications using high speed LEDs have been reported [21] and several optimizations to their setup are possible for higher bandwidth operation.

III. AUTO-CONFIGURABLE FSO NODE DESIGN

Auto-configurability of our FSO systems is based on two fundamental design components: (i) spherical surface tessellated with transceivers, and (ii) auto-alignment circuitry. As shown in Figure 2, the spherical surface provides angular diversity in receiving/transmitting optical signals in a virtually omni-directional manner, and the auto-alignment circuit selects which transceiver to use for data communication. We now detail these two components in the following subsections.

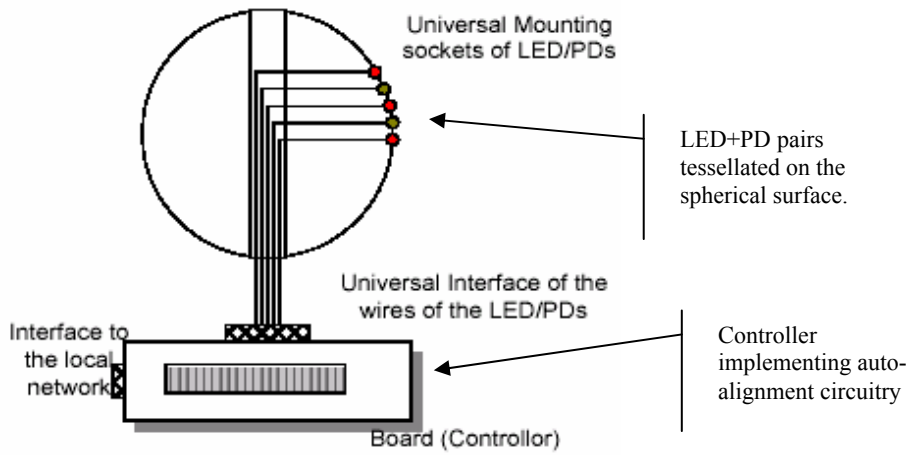

Figure 2: A schematic of the 3-d spherical FSO node design: Spherical surface is tessellated with LED+PD pairs, and an auto-alignment circuit is implemented on the controller of the system.

A. The Concept of Tessellated Spherical Surfaces

The geometric shape of a sphere suggests *spatial reuse* and *angular diversity*. We tessellated the surface of the sphere using optical transceivers each of which contains an LED (Light Emitting Diode) as the transmitter and a photo detector (PD) as the receiver. Since LEDs have relatively high divergence angle and PDs have a comparable angular field of view, the LED-PD pair forms a transceiver cone. This cone covers a significant volume of 3-dimensional space. As shown in Figure 1-(b), a sphere tessellated to an appropriate density can cover entire 360^0 steradian of the surrounding space. As seen from the Figure 3, when the spheres move relative to each other, an existing LOS between them is lost and a new one is established.

B. Auto-alignment Circuit

The basic functionality of the auto-alignment circuit is to monitor the incoming light beams at each transceiver and maintain continuous communication between two mobile FSO nodes by dynamically latching appropriate transceivers within their LOS. Figure 4 shows the schematic of the circuit for two spherical FSO nodes with four transceivers.

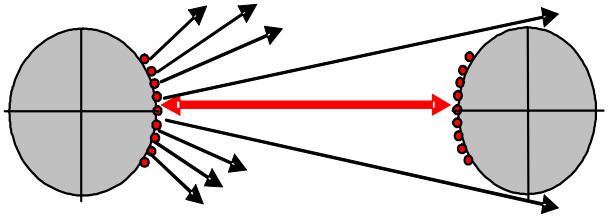

Figure 3: 3-d spherical FSO node showing a line of sight (LOS): Two spheres in LOS can potentially communicate even if they move in relation to each other. Even though LOS is lost at the previous transceivers, LOS can be quickly recovered through new transceivers located at other parts of the spheres.

In the event of misalignment, the circuit first (i) searches for an existing LOS between the two spheres, and then (ii) continues data communication through the new LOS, once a new LOS is established. These two functionalities are implemented in a common hardware for all the transceivers on a single spherical FSO node. The part of the circuit that monitors an existing LOS is shown as the "LOS Unit", which gives out a logical high output when an LOS is present between the two communicating nodes and a logical low input when the LOS is lost. The logical low output triggers the "LOS search". During this phase, data transmission is temporarily aborted and search pulses are sent out in all the directions looking for LOS. The second sphere, which now moved to a different location, also drops LOS and hence it too starts to initiate LOS searching. The spheres eventually receive the search pulses upon existence of a new LOS, which causes first a high output from the LOS Unit and then restoration of the data transmission.

For cases when multiple channels are aligned, we used a priority decoder to select a channel via the LOS signals from each transceiver. When no channel is aligned, the system searches for alignment by sending pulses to each channel. As soon as one or more channels get aligned, it starts

to send data signal out through the aligned channel. Thus, the logical data channel (or stream) is assigned to the physical channels dynamically depending on whether or not they are aligned. Several improvements (e.g. selection of the best transceiver when multiple ones are aligned) to this system are possible; however we are presenting a proof-of-concept experimentation in this paper.

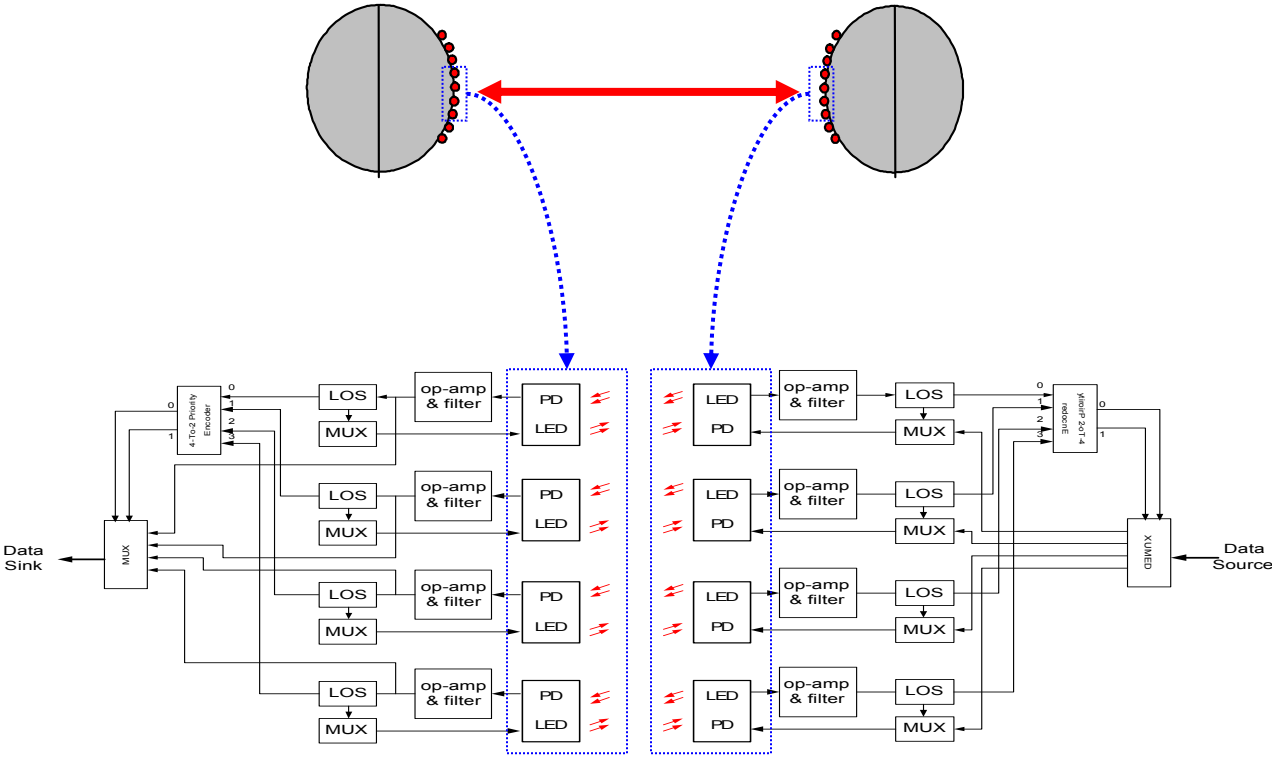

Figure 4: Schematic of the auto-alignment circuit with 4 physical channels: Four transceivers exist on each FSO node, and each of the four transceivers is connected to appropriate circuitry to automatically select the proper transceiver for communication in case of LOS.

IV. Mobility Analysis

We performed an experiment to demonstrate the concept of spatial reuse and LOS auto-alignment in the case when multi-channels are aligned. We built one cylindrical and one planar FSO node with 4 duplex optical channels on each. Each optical transceiver included an LED with a divergence angle of 24^0 and a PD with field of view of 20^0. We spaced four transceivers on the cylindrical surface (which projects as a circular line in 2-dimensions) with an equal separation angle φ of 32^0 along a circumference normal to the cylinder axis. The planar surface also included four transceivers equally spaced along a line.

Using the cylindrical and planar surfaces, we then placed the planar surface as part of a train's cargo, and moved the train along a circular path of radius 30cm around the cylindrical surface to create relative mobility. As the train moves the transceivers get aligned and misaligned. Figure 5-(a) shows a misalignment instance in which the search pulses are sent out by all transceivers and LEDs are glowing. Figure 5-(b) shows an instance of alignment in which two transceivers are in LOS with each other and data transmission is going through them. This pattern repeats as the train travels along the circular path. Figure 6 demonstrates the continuous alignment and misalignment phases as the train moves relative to the cylinder. For this setup, we used a light intensity threshold of 33.3lux at PDs to determine LOS. Notice that, LOS periods can be increased by appropriately tuning the light intensity threshold at PDs, the divergence angles of LEDs, the field of view angles of PDs, and by increasing tessellation density. The speed of the circuit should be more than the speed of the relative movement between the spheres so as to maintain a smooth data flow. Otherwise, the data will be either buffered or dropped. Design of such buffering and queuing techniques is an important research issue, which we will study in another paper.

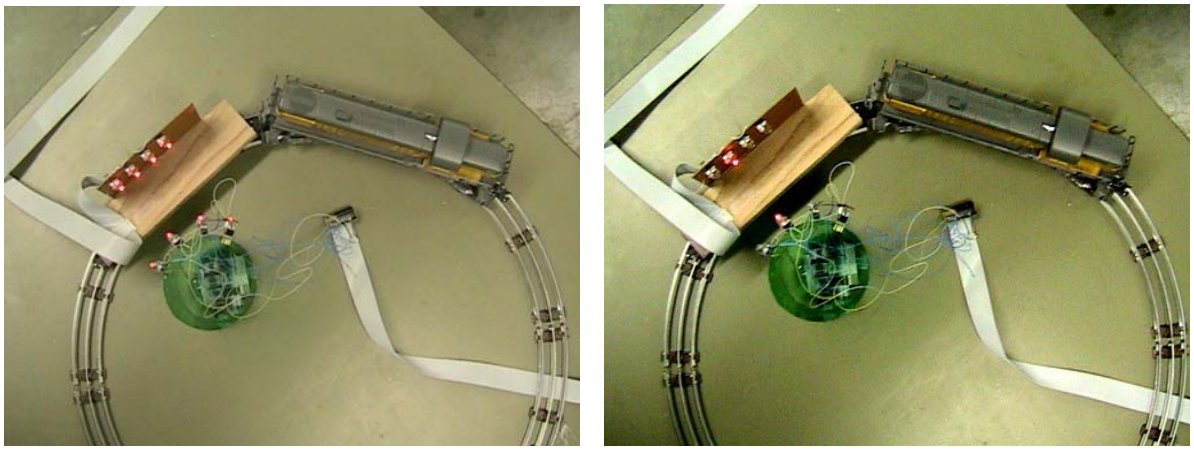

(a) Misaligned **(b) Aligned**

Figure 5: Illustration of the mobility experiment using a train: All transceivers are sending search pulses when LOS is lost as in (a). But, only the selected transceiver sends/receives when an LOS is detected.

To further analyze mobility in this experiment, we consider a train moving with an angular speed of ω radians/s. Given the light intensity profile in Figure 6, we can draw a generic LOS plot

as in Figure 7 for an LOS Detection Unit with a delay D seconds. Here, the length of alignment period will depend on LED's divergence angle θ and the train's speed ω; and the length of misalignment period will also depend on ω as well as density of tessellation which could be quantified as the angle φ during which alignment is lost. Notice that both θ and φ depends on LED's optical characteristics as well as the distance between the train and the stationary cylindrical FSO node.

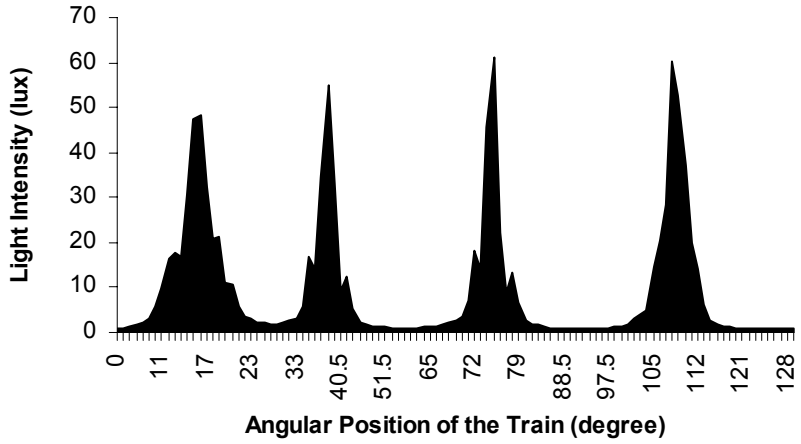

Figure 6: Intensity received at the cylindrical FSO node as the train moves along the circle.

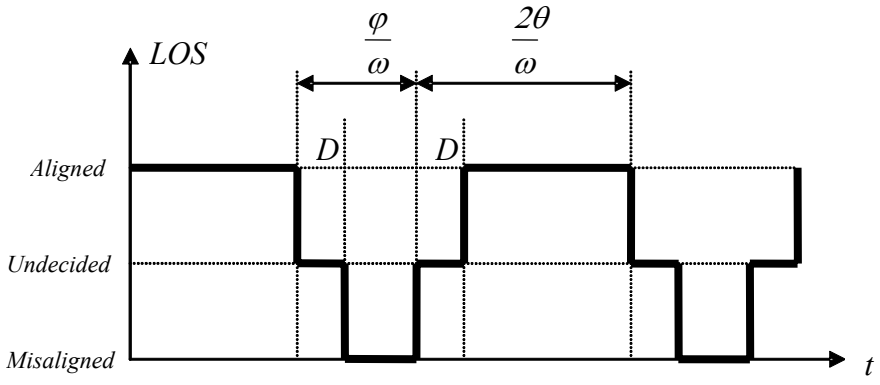

Figure 7: LOS condition with respect to a train moving with an angular speed ω.

Interestingly, in terms of the overall percentage of time the two FSO nodes are aligned, t_A, the train's speed will only affect the performance depending on the circuit delay. This relationship could be characterized as $t_A = \frac{2\theta - D\omega}{2\theta + \varphi}$. To observe effects of the circuit delay and mobility, we

have plotted t_A with respect to ω and D in Figure 8. We have chosen $\varphi = 0.5^0$ to see the behavior for a high density tessellation, and the divergence angle $\theta = 2^0$ as it can be approximated from Figure 6 for the LEDs we used. Notice the increased effect of mobility in performance when circuit delay is higher. It is worth noting that very high mobility is tolerable for very realistic circuit delay ranges, e.g. 50 degrees/s for less than 10 milliseconds circuit delay. Given that our experimental circuit had a delay about 200ns, this result shows practicality of high-density tessellation of optical transceivers.

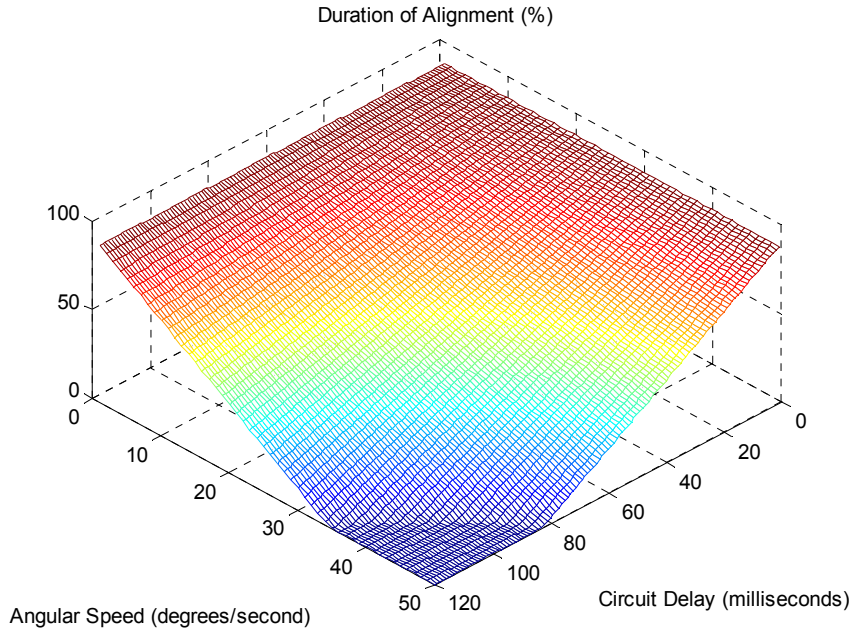

Figure 8: System performance with respect to train's angular speed.

V. Optimum Communication Coverage

Crucial characteristic of RF communication is that it allows connectivity through large communication coverage areas at all directions since RF signals are omni-directional. The *coverage area* here refers to the area around the node, in which a communication link can be established with another node standing within the area of consideration. Having large coverage areas compensates higher mobility and allows more flexibility to the mobile nodes. In this section, we will investigate maximum communication coverage areas that can be attained by our FSO

structures. Similar to RF, we will refer to coverage area as the area in which LOS and hence a communication link can be established with another spherical FSO node.

In spherical FSO nodes tessellated with multiple optical transceivers, there are tradeoffs involving (i) interference (or crosstalk) between the neighboring transceivers, (ii) aggregate coverage area achieved by the FSO node, (iii) packaging density of the optical transceivers, and (iv) communication range. Therefore, higher packaging density provides higher aggregate coverage but also increases the interference of the neighboring transceivers. An important design question is to ask how dense the packaging should be so that highest (or optimal) possible aggregate coverage is achieved without causing interference. In other words, what is the optimal number of transceivers to place on an FSO node to attain highest communication coverage? Another design tradeoff dimension is the communication range that can be achieved with such densely-packaged FSO nodes. If higher power is fed to the optical transmitters (e.g. LEDs) on the node, communication range increases; however, interference also increases at longer distances due to beam divergence. So, to investigate if the proposed FSO nodes can scale to long communication ranges, an analysis of how long communication ranges can be achieved is necessary.

In this section, to investigate the above-mentioned tradeoffs, we present our analysis of the scalability of the angular diversity and spatial reuse provided by a circular shaped FSO node. In particular, we answer the question of how much coverage can be achieved by a *2-d circular FSO node* with the highest possible number of transceivers. To find the optimal number of transceivers maximizing the total coverage of a 2-d circular FSO node, we first develop the model for total coverage area of such a node. Then, we devise an iterative algorithm to find the optimal number of transceivers that maximize the total coverage.

A. Coverage Model

We define the coverage area of an FSO node as the area in which another FSO node can be aligned for communication. Thus, the area, points of which are within the LOS of the FSO node, is called the *coverage area* of the FSO node under consideration.

For a 2-d circular FSO node, the total coverage is dependent on the effective coverage area achieved by a single transceiver C, and the total number of transceivers n. The effective coverage area of a single transceiver can be formulated based on two different possibilities of placing of the transceivers, as shown in Figure 9.

Let r be the radius of the circular 2-d FSO node, ρ be the radius of a transceiver, and θ be the divergence angle of a transceiver. We approximate an FSO transceiver's coverage area (which is the vertical projection of a lobe) as the combination of a triangle and a half circle. Let R be the height of the triangle, which means the radius of the half circle is $R\tan\theta$. Also, let τ be the length of the arc in between two neighboring transceivers on the 2-d circular FSO node.

Table 1: MATHEMATICAL NOTATIONS

Symbol	Meaning
n	Number of transceivers on the FSO node
r	Radius of the FSO node (cm)
ρ	Radius of a transmitter (cm)
τ	Arc length between two neighbor transceivers (cm)
θ	Divergence angle of a transceiver (Rad)
φ	Angular difference between two neighbor transceivers (Rad)
L	Coverage area of a transceiver (cm^2)
C	Effective coverage area of a transceiver (cm^2)
I	Interference area of two neighbor transceivers (cm^2)
R	Height of the triangle in the coverage area of a transceiver (cm)
$R_{\max}$	Maximum range reachable by the FSO node (cm)
P	Transmitter source power (dBm)
S	Sensitivity of the photo-detector receiver (dBm) (assumed -43dBm)
ς	Radius of the receiver (cm)
V	Visibility (km)
q	Particle distribution constant
λ	Optical signal wavelength (nm)
q	Particle distribution constant
x	Side angle of the upper isosceles triangle within the interference area (Rad)
k	Length of the base side of the upper isosceles triangle (cm)
y	Vertex angle seeing the intersecting arc of the interference area (Rad)

Assuming that n transceivers are placed at equal distance gaps on the circular FSO node, and since the diameter of a transceiver is 2ρ:

$$\tau = \frac{2\pi r - n2\rho}{n} = 2\left(\frac{\pi r}{n} - \rho\right) \tag{1}$$

From (1), the angular difference φ between two neighboring transceivers can be derived:

$$\varphi = 360^0 \frac{\tau}{2\pi r} \tag{2}$$

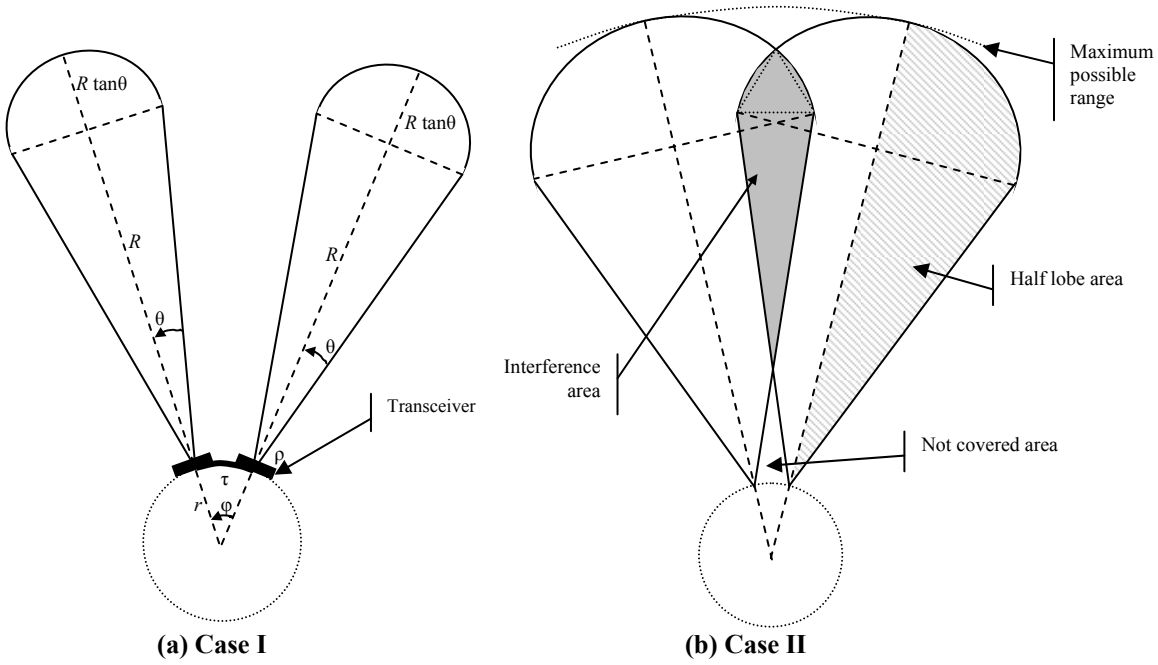

Figure 9: Coverage area of a 2-d circular FSO node: (a) Coverage areas of neighboring transceivers do not overlap. (b) Coverage areas of neighboring transceivers overlap.

Let L be the coverage area of a single transceiver, which can be derived as:

$$L = R^2 \tan\theta + \frac{1}{2}\pi(R\tan\theta)^2 \tag{3}$$

For the effective coverage area C of a single transceiver, two cases can happen based on the values of φ, θ, R, and r:

<u>*Case I:*</u> *Coverage areas of the neighbor transceivers do not overlap, i.e.* $R\tan\theta \le (R+r)\tan(\varphi/2)$. In this case, the effective coverage area is equivalent to the coverage area, i.e. $C = L$.

Case II: Coverage areas of the neighbor transceivers overlap, i.e. $R\tan\theta > (R+r)\tan(\varphi/2)$.

In this case, the effective coverage area is equivalent to the coverage area excluding the area that interferes with the neighbor transceiver. Let *I* be the interference area that overlaps with the neighbor transceiver's coverage, then $C = L - I$.

Notice that the interference area *I* is not fully useful for communication, since the signal the transceiver receiving is garbled by the presence of the signal from the adjacent transceiver(s) due to interference, unless we use WDM for the adjacent transceivers. LOS can still be achieved by selecting one of the transceivers for communication, however the other transceiver(s) receiving signal will be useless until the communication is over from the FSO node in the area *I*. Therefore, we do not count the area *I* in the coverage area, though this does not mean that those interference areas are totally ineffective.

How to calculate the interference area I? : As shown in Figure 9-(b), the interference area *I* is composed of two isosceles triangles and two leftover pies. To find the area *I*, the geometry for calculating the pieces of the area is needed. We need to find the angles *x* and *y*, and the length *k*, as shown in Figure 10. From Figure 10-(a), we can write the following relationships:

$$x + \frac{\varphi}{2} = \frac{180 - y}{2} \tag{4}$$

$$\frac{k}{2\cos x} = 2R\tan\theta\sin\left(\frac{y}{2}\right) \tag{5}$$

From (4) and (5), we find *x* and *y*, which means area of the upper isosceles triangle can be found. However, to do so, we still need to know the length *k*, which can be found by angles and lengths of the several triangles in Figure 10-(b):

$$k = 2\frac{R}{\cos\theta}\sin\left(\theta - \frac{\varphi}{2}\right) - 2r\sin\left(\frac{\varphi}{2}\right) \tag{6}$$

How to calculate the maximum range $R_{\max}$ *? :* Another important unknown is the maximum range $R_{\max}$ that can be reached by the 2-d FSO node. $R_{\max}$ is dependent on the transmitter's source

power P dBm, the receiver's sensitivity S dBm, the radius of the transmitter ρ cm, the radius of the receiver (on the other receiving FSO node) ς cm, the visibility V km, the optical signal wavelength λ nm, and the particle distribution constant q. FSO propagation is affected by both the atmospheric attenuation A_L and the geometric spread A_G, which practically necessitates the source power to be greater than the power lost [28].

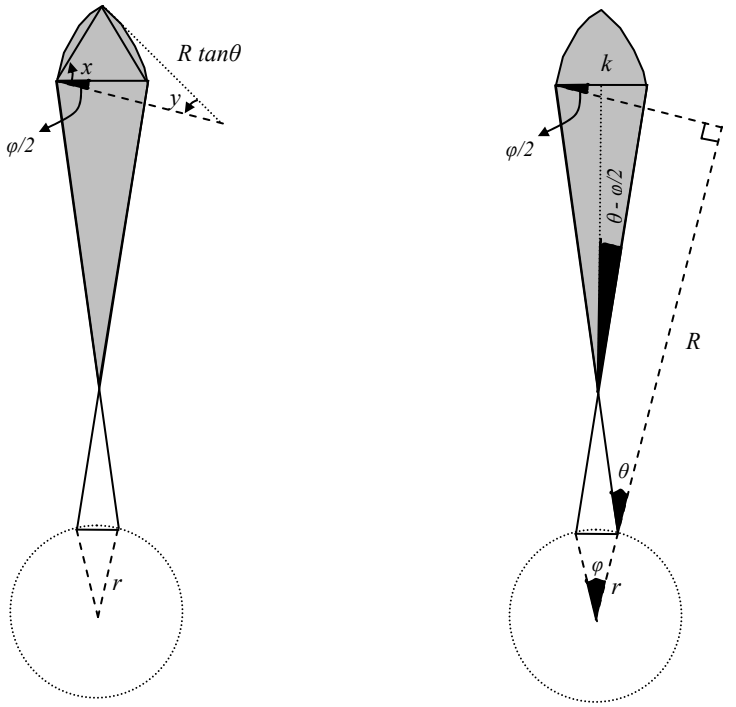

(a) Need to find the angles x and y. **(b)** Need to find the length k.

Figure 10: A few key angles and lengths need to be found to find the interference area.

Thus, for a conventional photo-detector (PD) sensitivity of S=-43dB, the following inequality must be satisfied for the PD to detect the optical signal:

$$S - P > A_L + A_G$$
$$-(P + 43) > A_L + A_G \quad (7)$$

Substituting A_L and A_G leads us to inequality, minimum solution of which is $R_{\max}$ [28]:

$$-(P + 43) > 10\log\left(e^{-\sigma R}\right) + 10\log\left(\frac{\varsigma}{\rho + 50R\theta}\right)^2 \quad (7)$$

where $\sigma = \frac{3.91}{V}\left(\frac{\lambda}{550}\right)^{-q}$. Note that after finding $R_{\max}$ from (7), the height of the triangle within the coverage area of a transceiver R can be found by $R_{\max} = R + R\tan\theta$.

B. Optimal Coverage

For given transmitter source power P, divergence angle θ, and visibility V, optimal number of transceivers that should be placed on the 2-d circular FSO node can differ. In particular, optimal number of transceivers (i.e. n) can be different based on the parameters P, θ and V as well as the metric to be optimized. We optimize the total effective coverage area nC of the 2-d circular FSO node, though other metrics (such as ratio of uncovered area and total possible area) can also be chosen. In addition to P, θ and V; the size of the FSO node (i.e. the radius of the FSO node circle r and the radius of a transceiver ρ) also plays a major role in the optimal number of transceivers n. Since C is dependent on P, θ, V and n; for given r and ρ, the optimization problem can be written as:

$$\max_{\theta,P,V,n}\{nC(\theta,P,V,n)\} \tag{8}$$

such that $0.1mRad \le \theta$, $P \le 32mW$, and $V \le 20{,}200m$.

Table 2: PARAMETERS FOR OPTIMIZATION

Parameter	Meaning	Value(s)		
		Min	**Max**	**Step**
θ	Divergence angle of a transceiver (mRad)	0.1	170	5
P	Transmitter source power (mW)	4	32	4
V	Visibility (m)	200	20,200	2,000
r	Radius of the FSO node (cm)	1	20	1
ρ	Radius of a transmitter (cm)	0.1	r/8	0.1

In our search for the best n, for a particular FSO node and transceiver size, we varied P, θ and V based on current FSO technology and literature, as shown in Table 2. We varied P from 4mW up to 32mW, as conventional lasers and LEDs use 4-10mW and 4-30mW respectively. Similarly, we

varied θ from 0.1mRad up to 170mRad, as lasers and LEDs have 0.1-100mRad and 139-240mRad respectively. Also, we varied the radius of the circular FSO node from 1cm to 20cm, which includes very small FSO node sizes (1-5cm of radius) for indoor usage as well as large sizes (10-20cm of radius) for outdoor usage. Finally, given a circular FSO node radius r cm, we varied the transmitter (or transceiver) radius from 0.1cm to $r/8$. This means for large FSO nodes (e.g. r=20cm) transmitter radius can be more than 1cm, which is larger than current LED sizes. However, it is possible to approximate large transmitter sizes by using a mesh of LEDs and PDs instead of a single LED and PD. Therefore, we do not deem this as a problem.

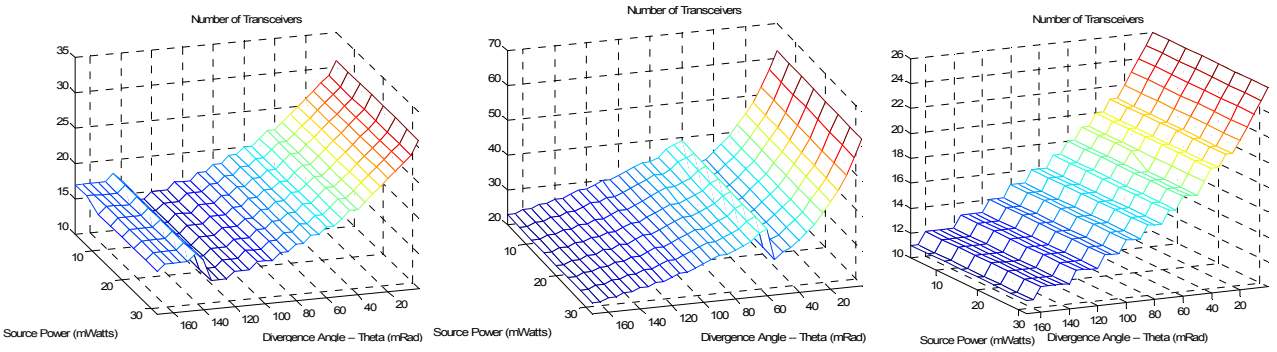

(a) r = 1cm, ρ =0.1cm **(b)** r = 20cm, ρ =1cm **(c)** r = 20cm, ρ =2.4cm

Figure 11: Optimal *n* for three different FSO nodes at all weather conditions: Source power and visibility have little or no effect on the optimality of n. The geometric shape of the FSO node and the divergence angle determine the optimality of the total coverage.

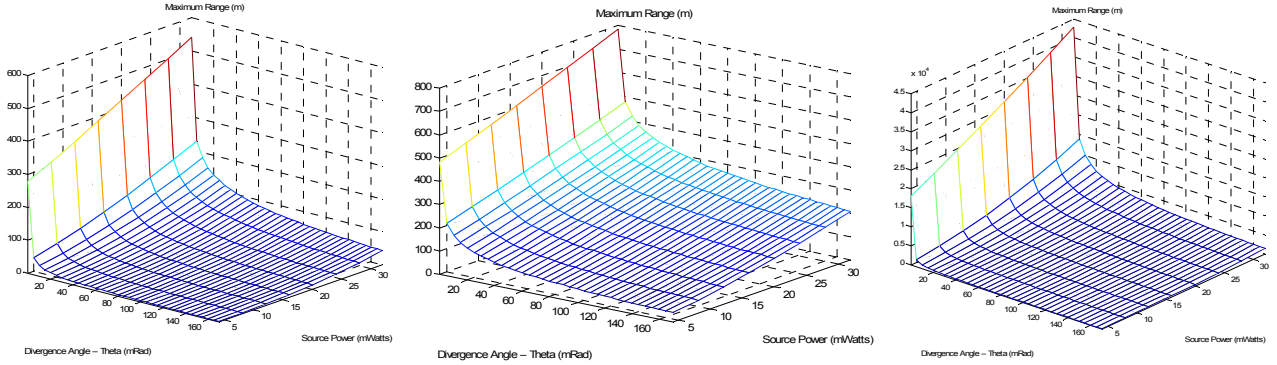

(a) r = 1cm, ρ =0.1cm, V=0.2km **(b)** r = 20cm, ρ =2.4cm, V=0.2km **(c)** r = 20cm, ρ =2.4cm, V=20.2km

Figure 12: Maximum communication range depends on all parameters affecting the FSO node design: Lower divergence angle or higher source power leads to higher communication range. Larger FSO node radius or transceiver radius leads to higher communication range.

C. Optimal Coverage Results

By applying the approach described in the previous section, we obtained optimal number of transceivers on a 2-d circular FSO node that maximizes the coverage area. To examine both small FSO node sizes (i.e. for indoors) and large sizes (i.e. for outdoors), we varied the FSO node radius *r* and the radius of a transmitter on the node ρ. Here, we report a subset of our results for the FSO node radius values of 1cm and 5cm for *indoors*, and 20cm for *outdoors*. Similarly, to examine different weather conditions, we varied the visibility *V*. We report a subset of our results for visibility of 0.2km for *adverse*, 6.2km for *normal*, and 20.2km for *clear* weather.

Figure 11 shows the optimal number of transceivers *n* for three FSO node designs (one for indoors, and two for outdoors) for all weather conditions. Notice that the optimal n values reported in Figure 11 are valid for all the three weather conditions (i.e. adverse, normal, and clear) we investigated. So, an interesting observation is that *the source power P and the visibility V have little or no effect on the optimality of n*; rather, the geometric shape of the FSO node and the divergence angle plays the major role. This is a very important result since it means that optimum number of transceivers is *fixed* for a particular FSO node and transceiver size regardless of the visibility and the source power situation. This property of circular or spherical (the property can be shown to be valid for 3-d spheres) *FSO nodes allows adaptive tuning of the source power based on the actual visibility*.

Furthermore, as can be seen from Figure 11, the relative size of the FSO node radius *r* and the transceiver radius ρ determines the shape of the optimal *n* as θ changes. Also, as expected, the optimal *n* reduces as θ decreases, though with steps at specific θ values corresponding to significant changes in the ratio of the interference area with respect to the total coverage area.

Another important metric for the FSO nodes is the maximum range R_{max} in which two such nodes can communicate. R_{max} depends on all parameters affecting the design. Particularly, lower θ or higher P leads to higher R_{max}, and larger r or ρ leads to higher R_{max}, as shown in Figure 12.

D. Design Recommendations

Value of the communication range, R_{max}, for various FSO node designs is very important as it shows scalability of our circular 2-d FSO node designs for long distances. As it can be seen from Table 3, *the maximum communication range of the node depends solely on the area of the transceiver* (i.e. the radius ρ) for fixed θ and P.

Table 3: MAXIMUM COMMUNICATION RANGE FOR OPTIMAL FSO NODE DESIGNS WITH θ=170.1mRad AND P=32mWatts.

Designs		Adverse Weather (V=0.2km)	Normal Weather (V=6.2km)	Clear Weather (V=20.2km)	Possible Usage
ID	**Node/Component Sizes**				
1	r = 1cm, ρ =0.1cm	43.29m	64.77m	65.69m	*Indoor*
2	r = 5cm, ρ =0.1cm	43.29m	64.77m	65.69m	*Indoor*
3	r = 5cm, ρ =0.6cm	121.23m	354.67m	382.24m	*Outdoor*
4	r = 10cm, ρ =0.1cm	43.29m	64.77m	65.69m	*Indoor*
5	r = 10cm, ρ =0.6cm	121.23m	354.67m	382.24m	*Outdoor*
6	r = 10cm, ρ =1.2cm	162.27m	646.88m	738.55m	*Outdoor*
7	r = 15cm, ρ =0.1cm	43.29m	64.77m	65.69m	*Indoor*
8	r = 15cm, ρ =1cm	151.00m	554.93m	622.42m	*Outdoor*
9	r = 15cm, ρ =1.8cm	188.44m	896.78m	1072.58m	*Outdoor*
10	r = 20cm, ρ =0.1cm	43.29m	64.77m	65.69m	*Indoor*
11	r = 20cm, ρ =1cm	151.00m	554.93m	622.42m	*Outdoor*
12	r = 20cm, ρ =2.4cm	207.82m	1115.88m	1387.21m	*Outdoor*

Table 3 provides the particular designs we investigated. We recommend some of these designs in for indoor usage (i.e. designs #1, #2, #4, #7, and #10) and other for outdoor usage (i.e. designs #3, #5, #6, #8, #9, #11, and #12). Though each design can serve a particular purpose based on the application, we marked the ones that we think fit best to indoor and outdoor usages. For example, designs #7 and #10 would be very good at using as a central hub attached to the ceiling of a crowded room as it can have lots of transceivers on it (i.e. ρ=0.1cm) while communication range

can be maintained at the order of 50m. Designs #1 and #2 would perform very well as a small device being attached to laptops or other mobile indoor devices where size of the system is not desired to be large. Similarly, designs #9 and #12 can be used at mobile nodes needing long-range (~1000m) outdoor communication, such as ships and flying objects like helicopters. Designs #6 and #8 seems best for medium-range (~100m) outdoor usage where another communicating node can be found within few hundred meters, as in for the cars or other mobile vehicles in a city.

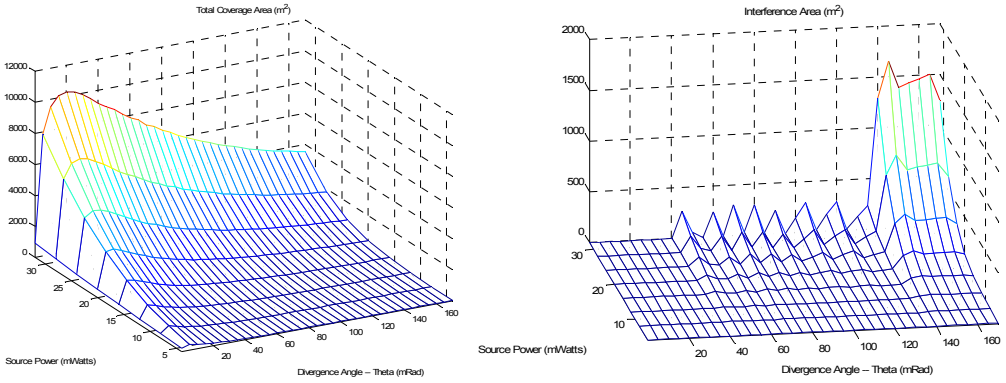

(a) Adverse weather, i.e. Visibility = 0.2km

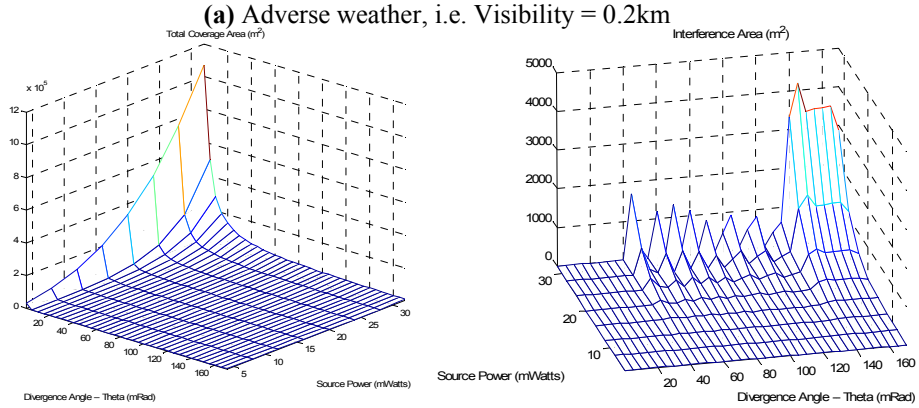

(b) Clear weather, i.e. Visibility 20.2km

Figure 13: Coverage area and interference area of an FSO node for *Indoor Design*, r = 1cm, ρ =0.1cm: When the divergence angle is very small, the transceiver radius ρ limits the maximum number of transceivers and no interference between neighbor transceivers exist. For higher divergence angles, maximum coverage can be obtained by having overlapping of coverage areas of neighbor transceivers as was shown in Figure 9-(b).

Table 3 also shows that our FSO node designs can scale up to 1387.21m as the communication range for outdoors. It is noticeable that this communication range can be achieved by an FSO node with radius 20cm covered with LEDs with divergence angle of 170.1mRad and source power of 32mWatts. Note that these divergence angle and source power values are within

the current technology limits of very cheap (e.g. $1 per piece) LEDs, and LEDs with better (lower divergence and higher power) can easily be produced with very small additional costs.

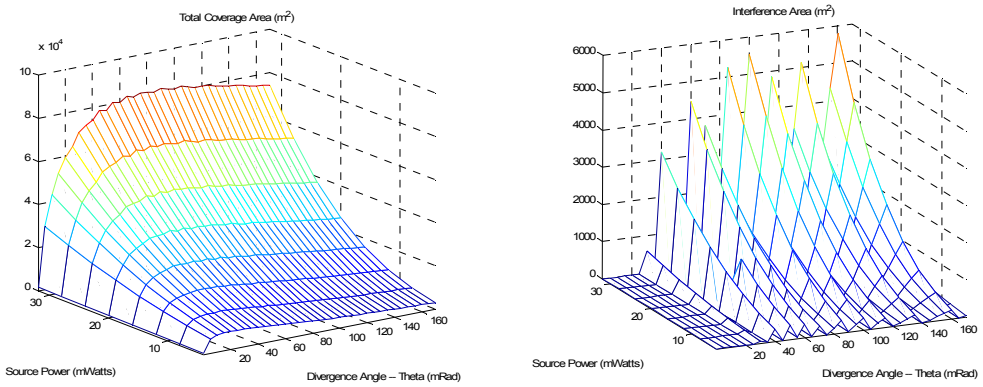

(a) Adverse weather, i.e. Visibility 0.2km

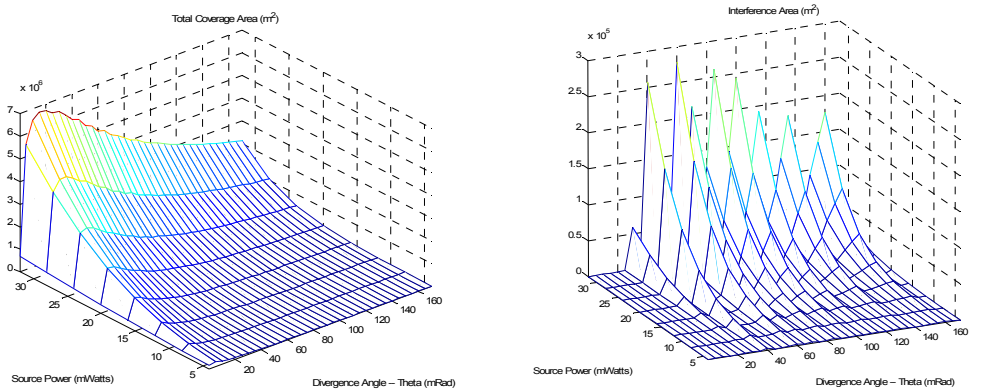

(b) Normal weather, i.e. Visibility 6.2km

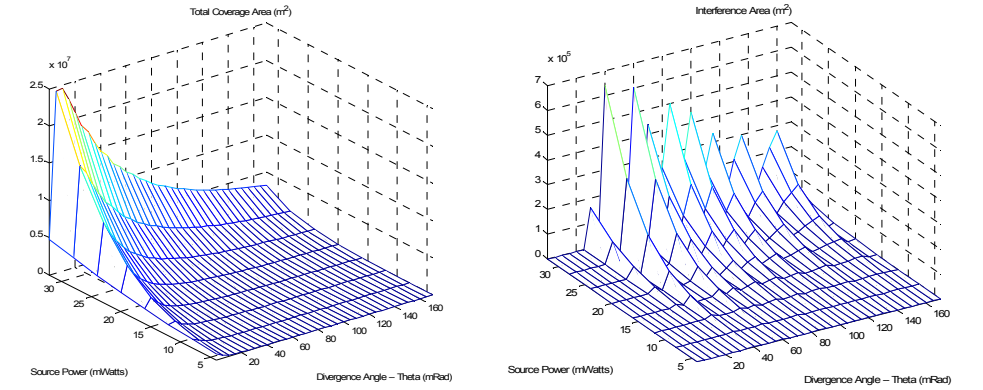

(c) Clear weather, i.e. Visibility 20.2km

Figure 14: Coverage area and interference area of an FSO node for *Outdoor Design*, r = 20cm, ρ =2.4cm: Similar to the indoor design, the transceiver radius ρ limits the maximum number of transceivers when divergence angle is small. Maximum coverage is achieved by having some interference of neighbor transceivers. Effect of changing the divergence angle is more severe on the coverage for more clear weather.

The total coverage nC area achieved by an FSO node also depends on the number of transceivers as well as the visibility, as shown in Figure 13. As can be seen from the behavior of

interference area in Figure 13, the optimal number of transceivers is dependent on several factors which help minimize the fraction of interference area with respect to the total coverage area. When the divergence angle is very small (i.e. θ<40mRad), the transceiver radius ρ limits the maximum number of transceivers (since $2\pi r \leq n2\rho$ must be satisfied) and hence no overlap exists between the coverage areas of neighbor transceivers. For θ values allowing possible overlap between neighbor transceivers' coverage, our optimization results in optimal *n* values causing interference areas as shown in Figure 13. Similarly, as shown in Figure 14, the same behavior of the interference area can be observed as no interference is seen for θ less than 20mRad.

As can be observed by comparing Figure 13-(a) and Figure 13-(b), the total coverage behaves differently in different weather conditions as θ varies. Our results show that, by using transceivers with radius 0.1cm and 32mRad source power, an FSO node with radius 1cm can cover a total of 2272.68m^2 in adverse weather and 5230.97m^2 in clear weather. *This result clearly shows scalability of our FSO node designs to very dense packaging of transceivers.* Similarly, by using transceivers with radius 2.4cm and source power 32mRad, outdoor size FSO node designs with radius 20cm can achieve a coverage area of 72,857.33m^2 in adverse weather, 2.10km^2 in normal weather, and 3.24km^2 in clear weather.

As shown in Figure 13 and Figure 14, an interesting result is that *effect of increasing θ on the total coverage is more severe for higher visibility cases*. This is due to the fact that FSO propagation constructs a lobe-like shape which means majority of the coverage area is farther away from the light source.

As shown in Figure 13 and Figure 14, the interference area corresponding for the FSO node design optimized for maximum communication coverage oscillates as the divergence angle varies. More specifically, as the divergence angle increases the interference area may or may not increase.

As explained in Figure 15, the reason is that fraction of interference area to the actual coverage area determines the optimality of the number of transceivers in the design.

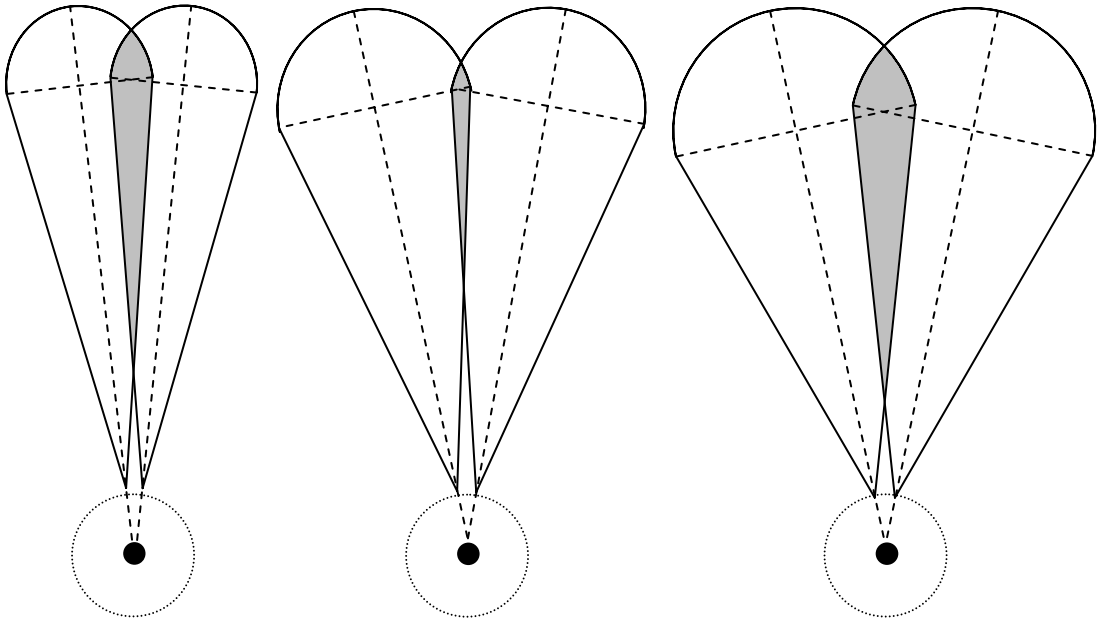

(a) Design I, θ_1, n_1 **(b) Design II,** θ_2, n_2 **(c) Design III,** θ_3, n_3

Figure 15: Optimal coverage and interference areas for different divergence angles are achieved by different number of transceivers: Divergence angles of the transceivers increase from Design I to III, i.e. $\theta_1 < \theta_2 < \theta_3$. However, optimum number of transceivers to maximize coverage may not necessarily decrease (e.g. $n_1 > n_2 = n_3$), which causes the interference area to be oscillating as divergence angles vary.

VI. SUMMARY

We proposed and developed a new scheme for mobile free space optical communications using (i) spherical surfaces tessellated with optical transceivers to obtain spatial reuse as well as angular diversity, and (ii) an auto-configurable optoelectronic circuit that makes use of this angular diversity to enable mobility between communicating nodes. The auto-configurable circuit monitors the LOS between two communicating spherical FSO nodes, and latches automatically onto existing LOS points. We built a proto-type system and demonstrated optical data transmission between mobile nodes. The basic techniques can be extended to configurations containing more than two nodes at longer distances. One key feature of our design is the absence of mechanical parts such as motors or moving mirrors typically used for auto-alignment purpose. This leads to

significant savings in power consumption and improved reliability of our modules. We showed, through two-dimensional modeling, that this kind of free-space-optical system designs allow very dense packaging, and can scale to very long communication ranges as well as large coverage. Future work includes issues like optimal transceiver packaging patterns for desired coverage in three-dimensions, and application-specific designs of such systems.

ACKNOWLEDGMENT

Authors would like to thank Mr. Chang Liu, Mr. Chingpo Chen, and Mr. David Partyka for thoughtful suggestions during various phases of this work.

This work is funded by NSF grant number NSF-STI 0230787.

REFERENCES

[1] S. Acampora and S. V. Krishnamurthy, "A broadband wireless access network based on mesh-connected free-space optical links," *IEEE Personal Communications* (October 1999), Volume 6, pp. 62 -65.

[2] J. W. Armstrong, C. Yeh, and K. E. Wilson, "Earth-to-deep-space optical communications system with adaptive tilt and scintillation correction by use of near-Earth relay mirrors", *Optics Letters* (Optical Society of America, Washington, DC, July 1998), Volume 23, Issue 14, 1087-1089.

[3] S. Arnon, "Effects of atmospheric turbulence and building sway on optical wireless-communication systems", *OSA Optics Letters* (January 2003), Volume 28, Issue 2, 129-131.

[4] S. Arnon and N. S. Kopeika, "Performance limitations of free-space optical communication satellite networks due to vibrations—analog case", *SPIE Optical Engineering* (January 1997), Volume 36, Issue 1, pp. 175-182.

[5] S. Arnon, S. R. Rotman, and N. S. Kopeika, "Performance limitations of free-space optical communication satellite networks due to vibrations: direct detection digital mode", *SPIE Optical Engineering* (November 1997), Volume 36, Issue 11, pp. 3148-3157.

[6] E. Bisaillon, D. F. Brosseau, T. Yamamoto, M. Mony, E. Bernier, D. Goodwill, D. V. Plant, and A. G. Kirk, "Free-space optical link with spatial redundancy for misalignment tolerance", *IEEE Photonics Technology Letters* (February 2002), Volume 14, pp 242 – 244.

[7] G. C. Boisset, B. Robertson., and H. S. Hinton, "Design and construction of an active alignment demonstrator for a free-space optical interconnect", *IEEE Photonics Technology Letters,* Volume 7, June 1999, pp 676 – 678.

[8] P. Djahani and J. M. Kahn, "Analysis of infrared wireless links employing multibeam transmitters and imaging diversity receivers Communications", *IEEE Transactions on Communications* (December 2000), Volume 48, pp. 2077 – 2088.

[9] G. E. F. Faulkner, D. C. O'Brien, and D. J. Edwards, "A cellular optical wireless system demonstrator", *IEEE Colloquium on Optical Wireless Communications*, 1999, pp 12/1-12/6.

[10] D. J. Goodwill, D. Kabal, and P. Palacharla, "Free space optical interconnect at 1.25 Gb/s/channel using adaptive alignment", *Optical Fiber Communication Conference, 1999,*

and the International Conference on Integrated Optics and Optical Fiber Communication. OFC/IOOC '99. Technical Digest, Volume 2, Feb 1999, pp 259 – 261.
[11] D. J. T. Heatley, D. R. Wisely, I. Neild, and P. Cochrane, "Optical Wireless: The story so far", *IEEE Communications* (December 1998), Volume 36, pp. 72 -74.
[12] K. Ho and J. M. Kahn, "Methods for crosstalk measurement and reduction in dense WDM systems", *IEEE/OSA Journal of Lightwave Technology* (June 1996), Volume 14, Issue 6, pp. 1127-1135.
[13] J. M. Kahn and J. R. Barry, "Wireless Infrared Communications", *Proceedings of the IEEE* (February 1997), Volume 85, pp. 265-298.
[14] D. Kedar and S. Arnon, "Backscattering-Induced Crosstalk in WDM Optical Wireless Communication". *IEEE/OSA Journal of Lightwave Technology* (June 2005), Volume 23, Issue 6, pp. 2023-2030.
[15] Lightpointe Inc., http://www.lightpointe.com/
[16] A. J. C. Moreira, R. T. Valadas, and A. M. O. Duarte, "Optical interference produced by artificial light", *ACM/Kluwer Wireless Networks*, Volume 3, pages 131-140, 1997.
[17] M. Naruse, S. Yamamoto, and M. Ishikawa, "Real-time active alignment demonstration for free-space optical interconnections", *IEEE Photonics Technology Letters,* Volume 13, Nov. 2001, pp 1257 – 1259.
[18] D. C. O'Brien, et al. "High-speed integrated transceivers for optical wireless", *IEEE Communications Magazine* (March 2003), Volume 41, pp 58 – 62.
[19] G. Pang, et al., "Optical Wireless based on High Brightness Visible LEDs", *IEEE Industry Applications Conference,* Vol. 3, pp. 1693 -1699, 1999
[20] A. Polishuk and S. Arnon, "Communication performance analysis of microsatellites using an optical phased array antenna", *SPIE Optical Engineering* (July 2003), Volume 42, Issue 7, pp. 2015-2024.
[21] R. Ramaswami, K. Sivarajan, *Optical Networks: A Practical Perspective*, Morgan Kaufmann Publishers, 2nd edition, 2001.
[22] B. E. A. Saleh, M.C. Teich, *Fundamentals of Photonics*, Wiley-Interscience, 1 edition, 1991.
[23] F. Shubert, Light-Emitting-Diodes-dot-org, http://www.rpi.edu/~schubert//Light-Emitting-Diodes-dot-org/
[24] A. Tavares, et al., "Experimental Characterization of Rate-Adaptive Transmission and Angle Diversity Reception Techniques". *IEEE Wireless Communications*, Vol. 10, No.2, April 2003.
[25] Terabeam Inc., http://www.terabeam.com/
[26] H. Uno, K. Kumatani, H. Okuhata, I. Shrikawa, and T. Chiba, "ASK digital demodulation scheme for noise immune infrared data communication", *ACM/Kluwer Wireless Networks*, Volume 3, pages 121-129, 1997.
[27] V. Vistas and A. C. Boucouvalas, "Performance Analysis of the Advanced Infrared (Air) CSMA/CA MAC Protocol for Wireless LANs", *ACM/Kluwer Wireless Networks*, Volume 9, pages 495-507, 2003.
[28] H. Willebrand and B. S. Ghuman, *Free Space Optics* (Sams Pubs, 1st edition, 2001).
[29] Y. E. Yenice and B. G. Evans, "Adaptive beam-size control scheme for ground-to-satellite optical communications", *SPIE Optical Engineering* (November 1999), Volume 38, Issue 11, pp. 1889-1895.
[30] X. Zhu, and J.M. Kahn, "Free-Space Optical Communication through Atmospheric Turbulence Channels", *IEEE Transactions on Communications*, August 2002.